

METHODOLOGY

Open Access



Optical measurement of tissue perfusion changes as an alternative to electrocardiography for heart rate monitoring in Atlantic salmon (*Salmo salar*)

Eirik Svendsen^{1,2*} , Finn Økland⁴, Martin Føre¹, Lise L. Randeberg³, Bengt Finstad⁵, Rolf E. Olsen⁵ and Jo A. Alfredsén¹

Abstract

Background: Welfare challenges in salmon farming highlights the need to improve understanding of the fish's response to its environment and rearing operations. This can be achieved by monitoring physiological responses such as heart rate (HR) for individual fish. Existing solutions for heart rate monitoring are typically based on Electrocardiography (ECG) which is sensitive to placement and electrode orientation. These factors are difficult to control and affects the reliability of the principle, prompting the desire to find an alternative to ECG for heart rate monitoring in fish. This study was aimed at adapting an optical photoplethysmography (PPG) sensor for this purpose. An embedded sensor unit measuring both PPG and ECG was developed and tested using anesthetized Atlantic salmon in a series of in-vivo experiments. HR was derived from PPG and compared to the ECG baseline to evaluate its efficacy in estimating heart rate.

Results: The results show that PPG HR was estimated with an accuracy of $0.7 \pm 1.0\%$ for 660 nm and $1.1 \pm 1.2\%$ for 880 nm wavelengths, respectively, relative to the ECG HR baseline. The results also indicate that PPG should be measured in the anterior part of the peritoneal cavity in the direction of the heart.

Conclusion: A PPG/ECG module was successfully adapted to measure both ECG and PPG in-vivo for anesthetized Atlantic salmon. Using ECG as baseline, PPG analysis results show that that HR can be accurately estimated from PPG. Thus, PPG has the potential to become an alternative to ECG HR measurements in fish.

Keywords: *Salmo salar*, Heart rate, Implant, Biosensors, Photoplethysmography

Background

Atlantic salmon (*Salmo salar*) is one of the most important species in fish farming with more than 2.6 Mt produced globally in 2019 [1]. A typical salmon production site consists of 8–10 flexible sea cages usually 50 m in diameter that holds a volume of around 40,000 m³. The

management and operation of such salmon farms entails a broad range of interrelated operations exerting convoluted effects on the fish. To ensure acceptable fish health and welfare conditions during production, relevant data to describe these must be collected and evaluated in conjunction with operational data. Such evaluations are largely subjective and experience based, and are carried out as part of the daily inspection and feeding routines.

About 15% of all farmed salmon are lost during production, a loss partly attributed to the lack of objective input to production control [2]. To address this loss,

*Correspondence: eirik.svendsen@ntnu.no

¹ Department of Engineering Cybernetics, NTNU, O.S. Bragstads Plass 2D, 7034 Trondheim, Norway

Full list of author information is available at the end of the article



© The Author(s) 2021. **Open Access** This article is licensed under a Creative Commons Attribution 4.0 International License, which permits use, sharing, adaptation, distribution and reproduction in any medium or format, as long as you give appropriate credit to the original author(s) and the source, provide a link to the Creative Commons licence, and indicate if changes were made. The images or other third party material in this article are included in the article's Creative Commons licence, unless indicated otherwise in a credit line to the material. If material is not included in the article's Creative Commons licence and your intended use is not permitted by statutory regulation or exceeds the permitted use, you will need to obtain permission directly from the copyright holder. To view a copy of this licence, visit <http://creativecommons.org/licenses/by/4.0/>. The Creative Commons Public Domain Dedication waiver (<http://creativecommons.org/publicdomain/zero/1.0/>) applies to the data made available in this article, unless otherwise stated in a credit line to the data.

recent research efforts have focused on determining what constitutes good fish welfare and which indicators one should quantify (i.e., measure) to obtain a more objective foundation for making welfare critical decisions [3], and safeguard ethically sound production. Sensing such indicators should be done using as unobtrusive measures as possible to avoid compromising safe and efficient operations. However, this is in conflict with the challenge of collecting data from a biomass contained in a volume of roughly 40,000 m³ of water, as this calls for distributed or mobile data collection systems which are based on, e.g., environmental sensing networks, sonars/echo sounders, passive acoustic monitoring and different types of optical methods such as underwater cameras [4]. Such systems are likely to be intrusive on the production, and may thus have to be removed from the aquaculture cage before operations are carried out to reduce the likelihood of, e.g., equipment damage. Furthermore, such technologies provide data with different spatial and temporal resolution and provide data on a population level since the recorded data are obtained from a sub-volume in the sea cage rather than from a specific group of fish. Sonars and cameras can provide data on a group level if smaller parts of the biomass are present within the sensor's field of view, a feature that has been used to estimate, e.g., fish size and cage biomass [5]. Although group and population level data can provide a certain insight into the dynamics in animal husbandry operations, the sensing technologies' intrusiveness on operations and limited understanding of the measurements' link to welfare imply that alternative or supplemental solutions for welfare evaluations are needed.

Individual level data provides the highest possible data resolution with respect to biomass, a feature recognized in precision farming both on land [6] and at sea [4]. In aquaculture, the main method for obtaining individual level data is using miniaturized, encapsulated electronic systems commonly referred to as "tags". Typical parameters that can be measured in an operational setting today are activity and swimming depth [7], heart rate (HR) [8], swimming speed [9] and position [10, 11]. Tags are available in two main types: Data storage tags (DSTs) and telemetry transmitter tags [12], and are usually surgically implanted into the fish's peritoneal cavity.

Tagging has been used successfully to study fish in different situations ranging from tracking fish in rivers and sea [13–15] to shedding light on fish behaviour in sea cages during aquaculture operations [7, 16]. Thus, tagged individuals may act as representatives (i.e., "sentinel fish") for the rest of the biomass in an aquaculture cage [17] to facilitate safer and less operationally intrusive welfare evaluations.

Changes in treatment and/or living conditions challenges an animal's homeostasis and may be expressed as various stress responses [18]. Recently, heart rate measured using DSTs was demonstrated as being linked to welfare [19] and stress [20] in Atlantic salmon and in other salmonids such as rainbow trout [21]. Heart rate may, therefore, serve as a proxy for stress, thereby providing information on the fish's welfare in aquaculture provided that heart rate can be obtained in real time. Heart rate estimates for fish are most commonly derived from an electrocardiogram (ECG) measured by electrodes integrated in the tag's encapsulation. However, the reliability of this method has been shown to be sensitive to tag deployment as the derived heart rate depends on the lateral placement in the fish as well as the tag's orientation [21]. Exploring other potentially more robust measurement principles for their ability to sense heart rate is, therefore, desirable, as it might contribute to making heart rate data more reliable and feasible to obtain for free swimming fish in aquaculture.

Photoplethysmography is an optical sensing technique quantifying changes in tissue perfusion (i.e., blood volume) by optical absorption. The photoplethysmogram (PPG) is a convolution of many components. In humans, slow-varying components may arise from breathing [22], while the superimposed pulsatile component changes with the cardiac cycle [23]. Using the pulsatile component from several wavelengths of light enables estimation of arterial blood oxygen saturation (*SpO2*) provided a mapping function compensating for tissue scattering effects is known [24]. Independent from this, the pulsatile component can be used to obtain a heart rate estimate as shown for both humans and other mammals [25, 26]. Thus, PPG is considered a likely candidate to address the challenges associated with ECG obtained using implants provided a suitable sensing solution can be designed.

Implantable PPG solutions have been developed for, e.g., sheep [27] and other mammals [28]. Although potentially relevant, such solutions are proprietary and either require additional, external interfaces for power and data collection/processing, or depend on radio-based data transfer, making them infeasible for use in fish in seawater. Measurement of PPG has been demonstrated for aquatic animals such as zebrafish (*Danio rerio*) using imaging PPG [29]. This is a suitable technique when tissues with low opacity can be remotely imaged in a controlled environment. This is the case for zebrafish in the larval stage, but not for Atlantic salmon in a context where using implants is considered relevant. Correspondingly, obtaining heart rate from PPG has been demonstrated by drilling holes and inserting PPG sensors through the shell of the Mediterranean mussel (*Mytilus galloprovincialis*) [30]. This

approach requires stationary subjects as the sensors are wired to external hardware for power and data logging. These approaches are, thus, not directly suited for fish implants, but demonstrate the feasibility of applying PPG for heart rate sensing for different aquatic animal groups.

In recent years a market desire for mobile medical equipment and consumer products containing such sensors (e.g., smart phones and sports watches [31, 32]) has driven development and miniaturization of PPG sensors. Such innovations have increased the potential to include such off-the-shelf sensors in implants for fish, as this is an application with similar requirements with respect to size and power consumption. However, the anatomical and optical tissue property differences between mammals and fishes, raise the question of whether PPG captured in Atlantic salmon using the common intraperitoneal implantation approach results in useful data. The purpose of this study was, therefore, to adapt an off-the-shelf PPG/ECG biosensing module for in-vivo testing in Atlantic salmon to investigate its potential to provide an alternative heart rate estimate from Atlantic salmon that does not suffer from the same limitations as ECG, while facilitating a future low-cost implant based on standard electronic components.

Methods

Sensing and logging equipment

The MAX86150 optical biosensor module [33] from Maxim Integrated (San Jose, USA) that offers both PPG and ECG output in a miniature package ($3.3 \times 5.6 \times \text{mm}$) with ultra-low power consumption, was selected for the measurements in this study. The physical and electrical properties of the module make it suitable for integration as the biosensor element of a prospective DST or acoustic tag with such sensing capability. A printed circuit board (PCB) was designed as a platform for miniaturizing the reference circuit design for the MAX86150. The PCB was subsequently cast in a cylindrical epoxy casing such that the sensing direction was perpendicular to the cylinder's longitudinal axis. Seven thin electrical wires protruded the rear of the cast and was used to extend the ECG electrode connections of the MAX86150, and to enable power connection and data transfer from the sensor. A battery powered MAX32630FTHR microcontroller board was used to relay data to a PC using Bluetooth. The cast also included a threaded aluminium end piece for attachment to a fixture rod. The fixture rod allowed horizontal and vertical sensor orientations as well as rotation of the sensor around its longitudinal axis. The complete assembly is shown in Fig. 1. Maxim DeviceStudio (V 5.3.03289.0) was installed on a Dell Latitude 7490

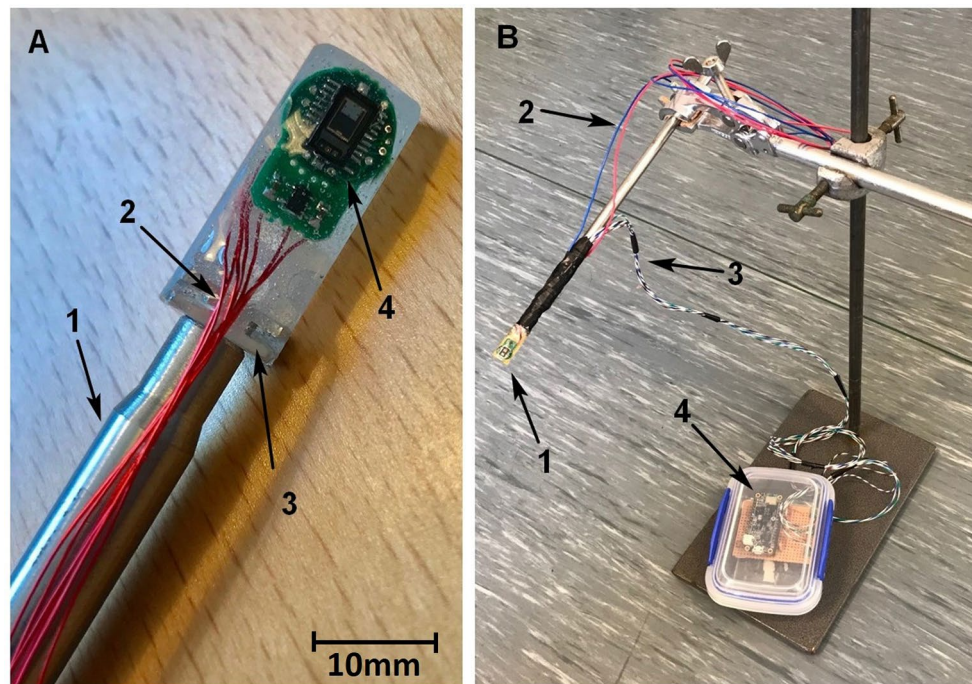


Fig. 1 **A** (left): 1. Fixture rod, 2. Wire extensions for MAX86150 ECG electrodes, power connection and data transfer, 3. Threaded aluminium end piece, 4. MAX86150 biosensor module. **B** (right): 1. Epoxy cast with MAX86150 biosensor module, 2. ECG electrode extension leads, 3. Data and power supply extension leads, 4. MAX32630FTHR microcontroller board for wireless data transfer to PC

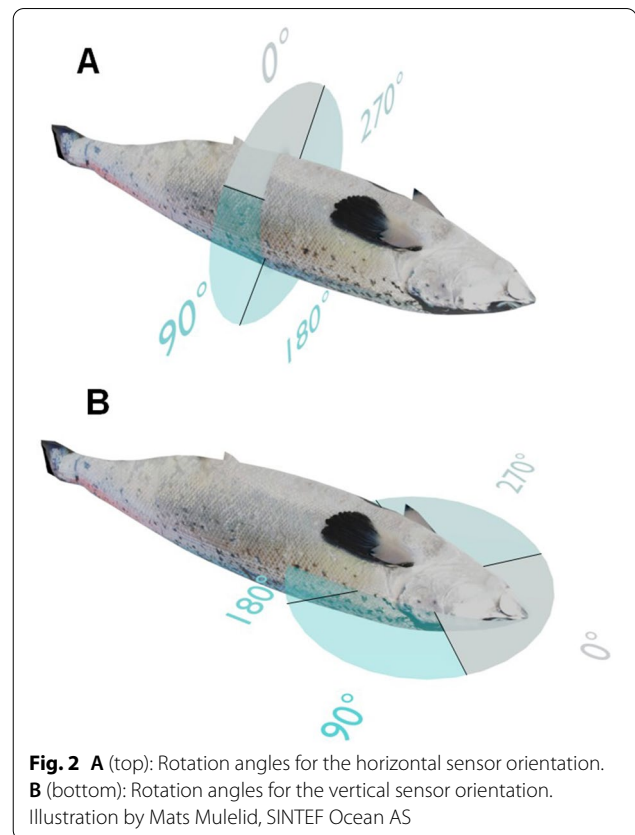
laptop computer and used for real-time data inspection and logging.

To determine the biosensor's feasibility when applied to Atlantic salmon, all sensor settings were kept the same for all data sets (sampling frequency $f_s=200$ Hz, RED (660 nm) and IR (880 nm) LED pulse amplitudes $A_{660}=A_{880}=20$ mA, LED pulse width $PW=400$ μ s, and no sample averaging), thus enabling signal quality comparisons across data sets. Note that when using PPG to estimate heart rate only, no reference measurements apart from the ECG baseline used for HR comparisons are required.

Experimental procedures

Individual fish were captured from a holding tank using a knotless dip net and immediately transferred to a tank containing water from the same water supply and anesthetic in a knock-out solution (70 mg l⁻¹ Benzoak Vet). The tank was covered using a Styrofoam plate after the fish was placed inside. Using a wheeled trolley, the tank was then moved to the indoor experimental location. When deemed to have reached level 3 anesthesia [34], the fish was placed in a specialized surgical table. By inserting a hose connected to a small pump into the fish's buccal cavity, continuously aerated water with maintenance anesthetic (35 mg l⁻¹ Benzoak Vet) was used to irrigate the gills and keep the fish sedated. The wire electrodes for ECG measurement attached to the MAX86150 were inserted into the muscle on the left and right lateral sides close to the heart. A 1–2 cm incision was made in the abdominal wall along the sagittal plane just anterior of the pelvic fins (position 1, Fig. 2A). For position 1, the sensor was inserted horizontally into the peritoneal cavity and one data set collected for orientations of 0° (ventral), 90° (right lateral), 180° (dorsal), 270° (left lateral) and 0° (ventral repeated) degrees rotation, respectively (Fig. 2A). Following data collection in position 1, a second 1 cm incision was made in the abdominal wall along the sagittal plane just posterior from the transverse septum (position 2, Fig. 2B). For position 2, the sensor was inserted vertically into the peritoneal cavity and one data set collected for orientations of 0° (anterior), 90° (right lateral), 180 degree (posterior), 270 degree (left lateral) and 0° (anterior repeated) degrees, respectively (see Figs. 2B and 3). Data was collected for 1 min for both positions and all orientations for each individual (10 data sets per fish / 50 data sets in total), after which the fish was euthanized by an anesthetic overdose (>70 mg l⁻¹ Benzoak Vet) and exsanguination.

A total of 7 fish were used for the experiment. No valid data was obtained for the first fish due to electrical interference likely caused by a nearby water pump



preventing valid ECG signals. Data collection was successful from the remaining 6 fish (from now on referred to as Fish 1 through 6), resulting in 10 data sets for fish 1, 2, 4, 5 and 6, and 6 data sets for fish 3 which suffered cardiac arrest after 6 data sets. The analyses were thus based on 56 data sets in total.

Data processing

Valid 20 s data subsets were manually selected and labelled based on the data evaluation criteria presented by Elgendi [35]:

- Salient ECG baseline.
- Salient PPG signal for one or both wavelengths.
- Similar PPG waveform morphology throughout the entire subset.

Data analysis using Python 3.8 (Anaconda Inc., Austin, Texas, USA) could then be conducted for valid data sets labelled “GOOD” (accept) or “FAIR” (accept). Data sets labelled “BAD” (reject) were judged to not contain the required information for signal quality calculations and were, therefore, omitted from further analysis. A complete overview of data sets and corresponding wavelengths considered valid based on these criteria is given in Table 1, while representative samples of PPG data sets labelled “GOOD”, “FAIR” and “BAD” can be seen in Fig. 4.

The default filtered ECG signal output from the MAX86150 was used to find HR by first scaling the filtered output to [0, 1] and then running a peak detection algorithm. Scaling was done so the same peak detection parameters for all ECG time series could be used. Peaks were identified using the “find peaks()” method in Python’s statistics module utilizing both a time window (i.e., the minimum required distance between peaks) and a prominence limit to identify the QRS peaks (i.e., ventricle depolarization) [36]. The time window was set to 160 samples (i.e., 0.8 s) based on a maximum expected HR of 80 BPM for Atlantic salmon [37] and comparable species [21]. Prominence was set to 0.4, thus demanding that the

QRS peaks were 40% higher than neighbouring peaks. HR was then determined by the average time difference (Δt_{avg}) between peaks using:

$$\text{HR}_{\text{BPM}} = \left(\frac{1}{\Delta t_{\text{avg}}} \right) \cdot 60 \quad (1)$$

Because raw PPG data containing both a stochastic trend and measurement noise was logged, a preprocessing step to remove these was necessary. The slow-varying (i.e., low-frequency) trend was removed using a third order Butterworth highpass filter [38] with a cutoff frequency of 0.25 Hz. Measurement noise was reduced using a second-order Savitzky-Golay filter [39] with a 50 sample (i.e., 0.25 s) window. This window size was chosen to retain as much information in the signal as possible based on the lowest expected HR of 15 BPM for Atlantic Salmon [37] and comparable species [21]. An example illustrating the result of these processing steps is given in Fig. 5. HR from PPG was then calculated from the detrended and noise suppressed signal using autocorrelation defined by:

$$y(m) = \sum_{n=1}^N X(n)X(n+m) \quad (2)$$

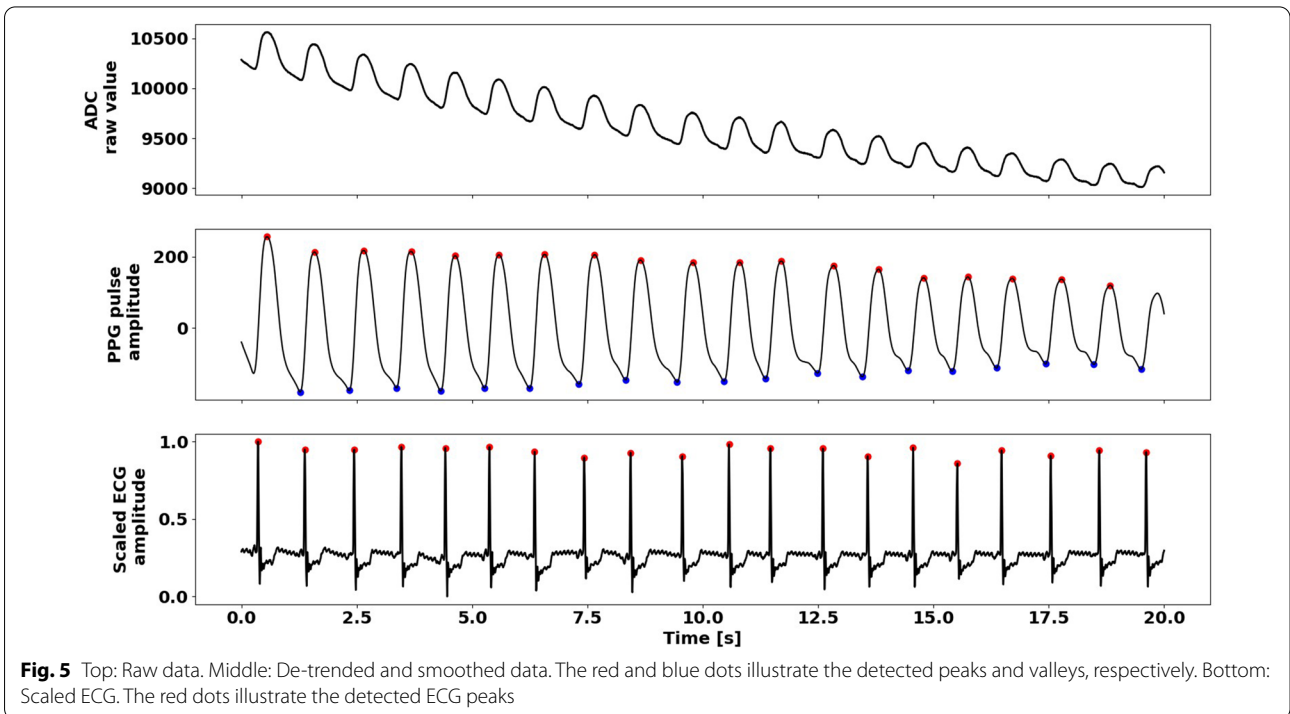
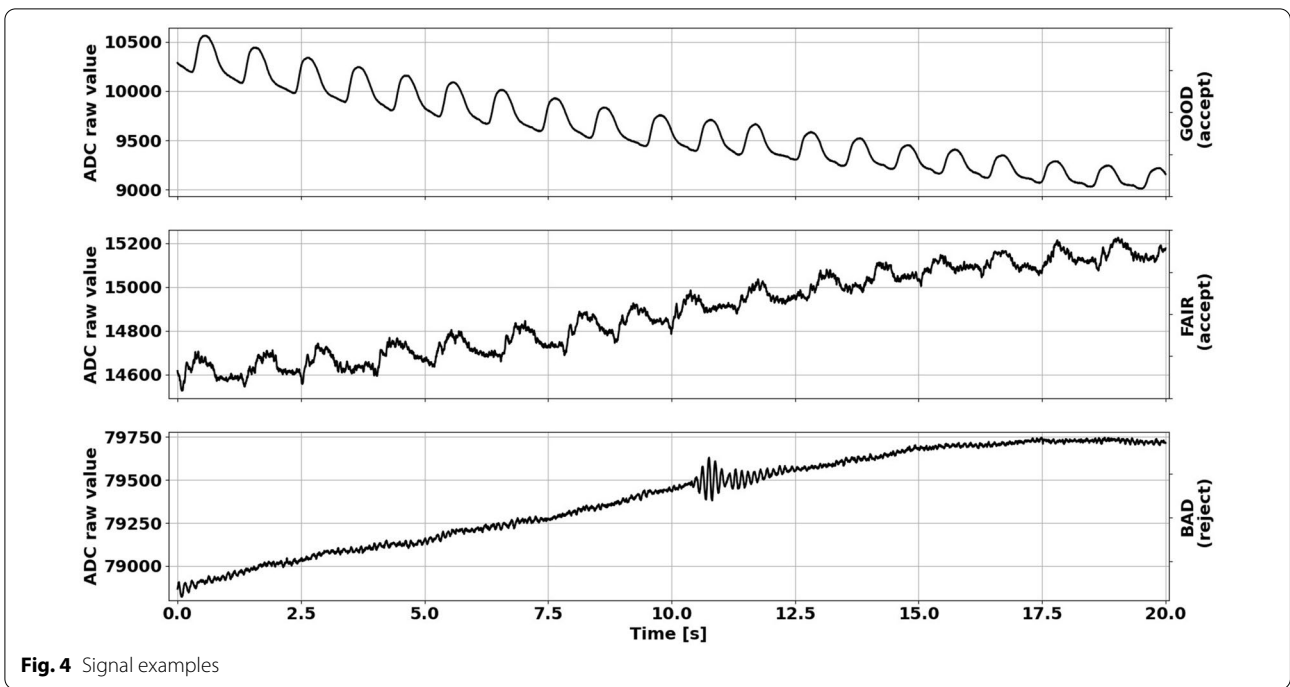
where N is the number of samples in the signal X , and $m \in [0, N-1]$. By applying the same peak detection method as that used for ECG, the index of the dominating peak (i.e., the first peak) in the autocorrelation series was identified. Because the autocorrelation series featured softer (but not flat/diffuse) peaks compared to the ECG signal, the prominence setting in the peak detection algorithm was relaxed to 0.3 to avoid too

Table 1 Summary of data set evaluations for both orientations, “Or.” (Hor = horizontal and Ver = vertical) and all rotations, “Rot.” (see Fig. 2) for all fish

Or.	Rot.	Fish1	Fish2	Fish3	Fish4	Fish5	Fish6
Hor 1	0	NVD	NVD	λ_2	NVD	λ_2	NVD
Hor	90	NVD	NVD	λ_2	NVD	NVD	NVD
Hor	180	NVD	NVD	λ_1, λ_2	NVD	λ_2	NVD
Hor	270	NVD	NVD	λ_1, λ_2	NVD	λ_1, λ_2	NVD
Hor 2	0	NVD	NVD	λ_1, λ_2	NVD	NVD	NVD
Ver 1	0	λ_1, λ_2	NVD				
Ver	90	λ_1, λ_2	λ_1, λ_2	N/A	λ_1, λ_2	NVD	λ_1, λ_2
Ver	180	λ_1, λ_2	NVD	N/A	NVD	NVD	NVD
Ver	270	λ_1, λ_2	λ_1, λ_2	N/A	λ_1, λ_2	λ_1, λ_2	λ_1, λ_2
Ver 2	0	λ_1, λ_2	λ_1, λ_2	N/A	λ_1, λ_2	λ_1, λ_2	λ_1, λ_2

NVD signifies “No Valid Data”, i.e., no part of the time series fulfils all selection requirements. λ_1 and λ_2 represents valid data for 660 nm and 880 nm, respectively

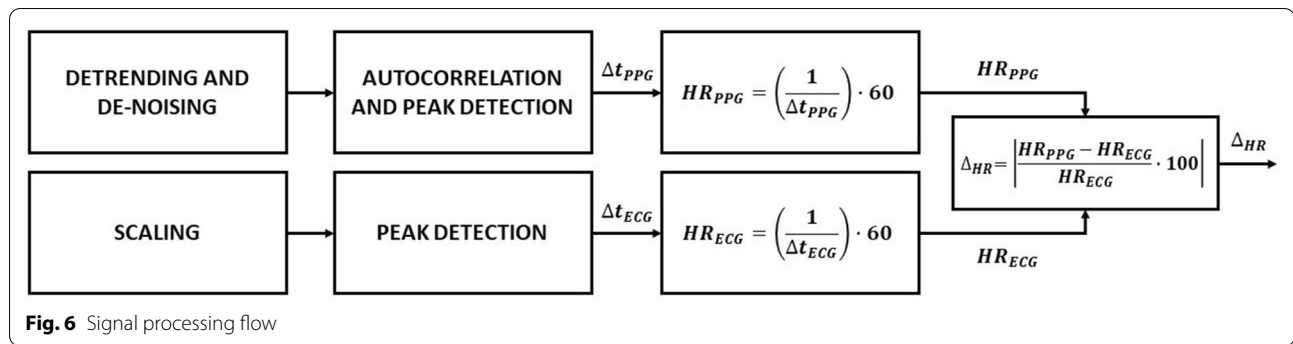
“N/A” (Not Applicable) denotes the data series which could not be collected for Fish 3 due to cardiac arrest. Note that the 0 degrees measurement has been repeated for both orientations



aggressive peak rejection. As for ECG HR, the time window was set to 160 samples. The index of the identified peak, therefore, represented the average time delay between peaks in the PPG time series, and was used to

calculate PPG HR in beats per minute (HRBPM) using Eq. 1.

To evaluate which sensor orientation and rotation gave the highest quality data, the signal quality index (SQI) for



the noise suppressed (but not de-trended) PPG signals, was calculated. SQI is defined for individual PPG pulses by [35]:

$$P_{SQI} = \frac{PPG_{pa}}{PPG_{avg}} \cdot 100 \quad (3)$$

where PPG_{pa} is the peak-to-peak PPG pulse amplitude and PPG_{avg} its mean value. The PPG signal where only noise suppression had been applied was used to retain access to the pulses' mean value which was removed during de-trending. A pulse was defined as the valley to valley noise suppressed data subsets. Valley indices (i.e., positions) were identified by inverting the de-trended (i.e., mean-centered) signal and reapplying the peak detection algorithm with the same window and prominence settings as those for autocorrelation peak detection. Using the valley indices, the pulses were extracted from the noise suppressed (but not de-trended) data sets, and the average SQI (SQI_{avg}) for all pulses calculated to represent the subset SQI. An example illustrating the peak detection result is given in Fig. 5.

To evaluate the accuracy of the PPG HR estimates, the difference between the ECG baseline and both wavelengths separately were calculated in percent using:

$$\Delta_{HR} = \left| \frac{HR_{PPG} - HR_{ECG}}{HR_{ECG}} \cdot 100 \right| \quad (4)$$

The signal processing flow is illustrated in Fig. 6.

Results

ECG was labeled “GOOD” in all data sets, while one or both PPG wavelengths were judged to qualify as “GOOD” or “FAIR” in 28 data sets. Thus, 28 (of 56) data sets were omitted from analysis. The results from the data processing are given in Table 2. The results show an average accuracy of $0.7 \pm 1.0\%$ for 660 nm and $1.1 \pm 1.2\%$ for 880 nm wavelengths relative to the ECG HR baseline. The average SQI (SQI_{avg} column in Table 2) indicates that the vertical orientation and 0 degrees rotation (i.e., measuring towards the heart) resulted in the best data quality.

Discussion

The high accuracy for HR computed from PPG compared to the ECG baseline from our experiments indicates that PPG is a viable alternative sensor principle for monitoring heart rate in Atlantic salmon. Moreover, the MAX86150 unit appears to be a suitable sensor module for implementation in future DSTs or transmitter tags aiming to measure and report HR over time. Although the sensor is designed for integration in optical HR measurement applications for humans and, thus, with human tissues and blood in mind, the HR estimate relies solely on the time-varying tissue perfusion. While human and fish blood is different with respect to composition and cell morphology, the essential functionality is the same, as is the hemoglobin [40]. The wavelengths emitted by the MAX86150 sensor are chosen due to their absorption sensitivity to oxy- and deoxyhemoglobin which determines the blood's oxygenation and thus its colour. Because tissue colour is affected by perfusion, processing either or both wavelength will be a feasible approach to obtain HR in both humans and fishes.

The data used in this study originates from 6 different fish, yielding 28 data sets. Although up to 10 data sets were collected from each fish, the data sets are considered independent because each data set is separate in either time, relates to different tissues, or both. When reviewing Table 1, most data available for processing came from the anterior part of the fish. This is probably because the measurements in this region coincide with locations with a high blood supply such as the liver and gut (thus implying high perfusion) compared to the posterior region where tissues with lower perfusion (mostly white muscle tissue) are present. This is supported by that the average SQI (Table 2) was highest for locations and orientations associated with the anterior part of the fish, especially for the 0 degree rotation which is towards the heart. This indicates that future implementations of PPG sensors for Atlantic salmon should facilitate data collection in this area.

Table 2 Results sorted by average SQI where the columns named Fish is the fish number, Or. is the orientation, Rot. is the rotation, HR_{ECG} is the heart rate in BPM calculated from ECG, HR_{660} is the calculated heart rate in BPM for the 660 nm time series, HR_{880} is the calculated heart rate in BPM for the 880 nm time series, ΔHR_{660} is the difference in HR estimate between the 660 nm time series and ECG in percent, ΔHR_{880} is the difference in HR estimate between the 880 nm time series and ECG in percent, SQI_{660} is the SQI for 660 nm, SQI_{880} is the SQI for 880 nm and SQI_{avg} is the average SQI, respectively

Fish	Or.	Rot.	HR_{ECG}	HR_{660}	HR_{880}	ΔHR_{660}	ΔHR_{880}	SQI_{660}	SQI_{880}	SQI_{avg}	Likely tissues
5	Ver	270	50.4	50.2	50.4	0.40	0.00	0.03	0.02	0.02	M, F
3	Hor 2	0	53.1	53.3	53.3	0.38	0.38	0.04	0.05	0.05	F
5	Hor	270	50.6	50.4	50.6	0.40	0.00	0.02	0.08	0.05	M, F
5	Hor 1	0	35.9	N/A	35.2	N/A	1.95	N/A	0.08	0.08	F
5	Hor	180	46.0	N/A	46.0	N/A	0.00	N/A	0.10	0.10	F, I
2	Ver	270	43.0	42.7	42.4	0.70	1.40	0.16	0.14	0.15	M, F
5	Ver 1	0	49.0	48.6	48.2	0.82	1.63	0.28	0.06	0.17	L, G
3	Hor	90	41.1	N/A	40.7	N/A	0.97	N/A	0.18	0.18	M, F
3	Hor 1	0	41.1	N/A	40.7	N/A	0.97	N/A	0.18	0.18	F
3	Hor	180	41.7	41.2	41.0	1.20	1.68	0.21	0.21	0.21	F, I
6	Ver	90	27.5	27.3	26.8	0.73	2.55	0.36	0.17	0.26	M, F
3	Hor	270	42.9	42.9	43.5	0.00	1.40	0.48	0.24	0.36	M, F
5	Ver 2	0	52.6	52.6	52.6	0.00	0.00	0.48	0.25	0.36	L, G
4	Ver	270	37.7	37.7	37.9	0.00	0.53	0.81	0.51	0.66	M, F
2	Ver	90	35.0	35.1	35.2	0.29	0.57	0.95	0.74	0.84	M, F
6	Ver	270	36.0	35.8	35.7	0.56	0.83	1.51	0.55	1.03	M, F
2	Ver 2	0	48.6	48.8	48.8	0.41	0.41	0.87	1.59	1.23	L, G
1	Ver	270	18.0	18.2	18.2	1.11	1.11	2.35	0.63	1.49	M, F
1	Ver	90	13.9	13.8	13.8	0.72	0.72	1.95	1.24	1.60	M, F
1	Ver	180	19.0	18.9	18.9	0.53	0.53	2.55	0.69	1.62	G, F
6	Ver 2	0	33.6	33.6	33.6	0.00	0.00	3.27	0.66	1.96	L, G
2	Ver 1	0	32.8	32.0	32.0	2.44	2.44	2.66	1.84	2.25	L, G
4	Ver 2	0	70.2	70.2	70.2	0.00	0.00	2.96	1.61	2.28	L, G
3	Ver 1	0	59.4	59.4	59.4	0.00	0.00	3.75	1.32	2.54	L, G
4	Ver 1	0	32.4	30.7	31.3	5.25	3.40	4.69	1.38	3.04	L, G
1	Ver 1	0	19.4	19.3	19.3	0.52	0.52	13.2	2.90	8.05	L, G
1	Ver 2	0	26.7	26.5	26.5	0.75	0.75	14.59	6.20	10.40	L, G
4	Ver	90	37.2	37.6	39.2	1.08	5.38	24.68	7.92	16.30	M, F

The table entry "N/A" (Not Applicable) is for the cases where no valid data could be identified for the respective wavelength in a particular data set. Entries in the Likely tissues column are: M: Muscle, F: Fat, I: Intestines, L: Liver and G: Gut, and denote tissues likely present in the sensing volume for the associated sensor orientation and rotation

The range between the lowest (13.9 BPM) and highest (70.2 BPM) heart rates may be explained by that different fish individuals would have had different physiological baselines (e.g., stress levels and health) prior to the experiments. These differences would, thus, have yielded different individual responses to handling and anesthesia. Differences in heart rates were, therefore, be expected. Reported heart rates for Atlantic salmon and comparable species are between 15 and 80 BPM [21, 37]. With the exception of one individual (13.9 BPM) all measured heart rates fell within this expected range. The individual having a heart rate below 15 could have been more susceptible to sedation thus explaining this result, or the reported HR range is conservative.

In our results, HR was reported using one decimal because additional decimal points are likely inaccurate. This conclusion stems from considering the HR-dependent quantification error for our highest HR (70.2 BPM). When sampling at 200 Hz, the change in BPM resulting from what is considered the maximum timely offset from true peak position can be calculated. This is achieved by first finding beats per second (BPS) which in this case is $70.2/60 = 1.17$ BPS. The time between HR peaks will in this case be $\Delta t = 1/1.17 = 0.855$ s. A timely offset in true peak placement exceeding 50% of the sampling interval implies that a peak will be associated with the previous or next sampling point. Hence, for our quantification error we get $Eq = 0.855 + (1/200) \cdot 0.5 = 0.8575$ s. This peak to

peak distance which includes the 50% offset, then gives a shifted BPM of $\text{BPM} = 60/0.8575 = 69.995$. The BPM difference can then be calculated as $\Delta\text{BPM} = 70.2 - 69.995 \approx 0.2$ BPM. The corresponding number for our lowest baseline HR (13.9 BPM) is 0.008 BPM.

The quantification error considerations are closely related to our measurements' sensitivity. By first accepting that a peak cannot be placed "between" two sampling points, the sensitivity can then be evaluated in the same way as the quantification error, only using the whole sampling interval. Thus, the sensitivity can be considered to be twice that of the quantification error, i.e., 0.4 BPM per sample offset for 70.2 BPM, and 0.016 BPM per sample offset for 13.9 BPM.

The deviation from the baseline of $0.7 \pm 1.0\%$ for 660 nm and $1.1 \pm 1.2\%$ for 880 nm can be explained by different factors. One potentially important source of error is that PPG is sensitive to motion artefacts. Such artefacts can be divided into two types: Perfusion changes in tissue caused by motion and relative motion between the sensor and the sensing volume. The former is not considered relevant when evaluating the results because all fish were in level 3 anesthesia (surgical) and, thus, motionless. However, such artefacts are likely to be important when the method is applied to free-swimming non-sedated fish. A logical next step on the path towards an operational measurement method would, therefore, be to apply the sensor to fish exhibiting normal swimming behaviour, and collect concurrent PPG and motion data to assess the potential impact of specific motion patterns.

To minimize the effect of the latter, the setup was designed to be as rigid as possible to ensure a stable sensing environment during data collection (Figs. 1 and 3). However, although the setup was mechanically stable and the fish in level 3 anesthesia, motion artifacts caused by potential tissue movement such as peristalsis [40] may have caused transient changes in the trend and potential changes in the amplitude of the PPG's pulsatile

component. This is partly remedied using high pass filtering in the analyses, as this effectually reduces or removes long term trends and any changes therein. Moreover, an estimate of HR relies solely on the frequency content in the PPG signal measurement signal, and not the amplitude. Based on these observations, movement of tissues relative to the sensor during data collection were unlikely to have had impact on the results.

Motion artefacts may also have been caused by tissue contraction (e.g., the heart) if it was within the sensing volume during data collection. This is particularly relevant for the vertical orientation with 0° rotation (i.e., when the sensor was pointing towards the heart). Because this is of particular concern, a subsequent post mortem dissection of Atlantic salmon was done to assess the sensing volume for this orientation and rotation. The dissection revealed that the tissue observed with the present method was likely dominated by low-perfusion fatty tissues surrounding larger blood vessels such as the hepatic arteries and veins (Fig. 7) [40]. Fat has a high optical scattering [41] coefficient due to lipid droplets inside the fat cells. Due to the size of the scatters, this scattering is highly forward directed and almost independent of the wavelength of the light. This implies that the light from the sensor is strongly scattered by the tissue while the intensity decays exponentially with distance from the light source in accordance with the (modified) Beer–Lambert law [42], thus limiting the distance light travels. This is indicated by the fact that the SQI for both wavelengths was generally low due to the big difference between the pulsatile PPG component's amplitude and the signal mean. A large mean value implies that a lot of light is scattered back to the receiver without having penetrated far into the tissue. It is, therefore, likely that the data originates from tissues close to the light source and that the heart is not part of the sensing volume.

Accuracy may also have been affected by the physiological state of the fish. The fish used in the experiment were

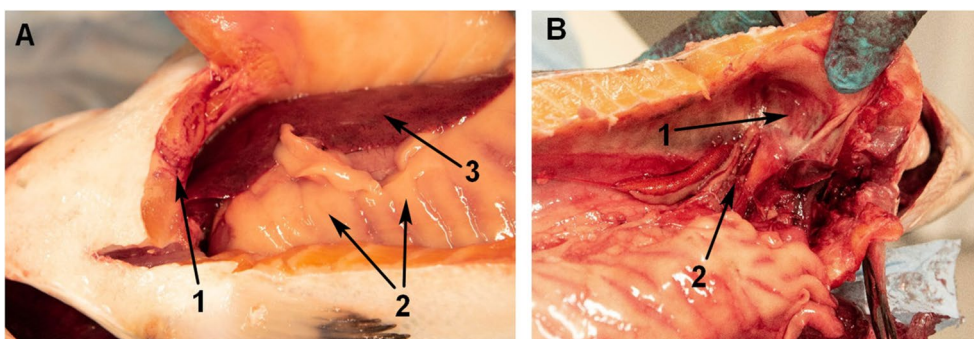


Fig. 7 **A** (left): 1. Epigastric vein/artery, 2. Pylorus caeca/lipid deposits, 3. Liver. **B** (right) 1. Septum transversum, 2. Hepatic arteries/veins

lab grown and showed no signs of deteriorated health. The anesthesia had both an analgesic and a paralyzing effect. It must, therefore, be expected that the secondary circulation system driven by the caudal heart and movement was impaired during data collection. In addition, the fish underwent a surgical procedure and the incisions as well as the sensor insertion may have further disturbed parts of the circulation system. When reviewing Table 2 for fish where data for both iterations of the horizontal and vertical 0° are available, similar SQIs for both iterations appear to be the trend. Although this indicates that the physiological state of the fish remained stable during data collection, it is likely that this state differs from that a fully awake and moving fish would exhibit. This underlines the necessity of conducting further experiments with fish exhibiting more normal behaviours and physiological function.

The peak detection procedure may have affected the accuracy of the method because the detrended PPG signals consisted of an oscillating curve with wide peaks compared to the ECG peaks. The accuracy in PPG peak detection was, therefore, lower, thus resulting in slight differences in the intervals between the detected PPG peaks and their corresponding ECG peaks. For long time series containing many peaks, such differences are expected to cancel out, but this may not have been the case for 20 s data sets. This may have been further exacerbated by the fact that the various orientations and rotations would have illuminated tissues and capillary beds supplied by haemal arches connected to different points along the dorsal artery. The resulting differences in pulse transit times (PTT, i.e., times between the heart beat and when it is observable in the sensing volume), may have shifted the PPG in relation to the ECG [43]. Furthermore, if different capillary beds with different PTTs were present in the sensing volume it could have distorted the PPG pulses by dragging them out in time, thereby explaining the differences in morphology seen between the “GOOD” and “FAIR” pulse examples in Fig. 4.

The criteria used for the selection of valid data subsets for analyses are subject to interpretation as highlighted by Elgendi et al. [35], meaning that other evaluators could have included some rejected data sets and vice versa. Although this is an inherent weakness in this method for assessing data quality, it is of greatest importance when using PPG for determination of *SpO2* where the PPG shape is paramount for the validity of the *SpO2* estimate [24]. When estimating HR only, PPG morphology is of lesser concern since only the frequency content of the pulsatile PPG component is required. The PPG based HR estimate is, therefore, considered robust against variations in interpretation of the subset selection criteria.

Autocorrelation was chosen for PPG analysis because its low computational demand and robustness against potential transient motion artifacts makes it a likely candidate for implementation in a microcontroller suitable for integration in a size and energy constrained fish tag. However, it cannot be ruled out that other, more computationally demanding approaches such as singular spectrum analysis [44], wavelet analysis [45] or a fast Fourier transform [46] approach could have given better results.

The perfusion index (Eq. 3) was used to evaluate signal quality because this is considered the “gold standard” for PPG signal quality evaluation, even though alternative methods (e.g., skewness, kurtosis and entropy) [35] which might lead to better results, exist. Such methods, however, are derived using reference data readily available for humans. To the authors’ knowledge, no reference PPG data for fish exist for comparison. Such data would be a very useful resource in developing new methods for quality evaluations of PPG data from fish, particularly if aspiring to quantify *SpO2*.

Overall, valid data was identified for all orientations and rotations. Although certain combinations of orientation and rotation yielded fewer data sets fulfilling the subset selection criteria than others, this does not necessarily mean that data are harder to obtain for these orientations and rotations. The same low-energy output settings were used for both orientations and all rotations, thus implying that more valid data could have been obtained if sensor settings, such as output power, had been increased. PPG, therefore, has the potential of being a robust alternative to ECG for HR measurement in fish.

Conclusions

A PPG/ECG module has been successfully adapted to measure both ECG and PPG in-vivo for anesthetized Atlantic salmon. Using ECG as baseline, results from an analysis of the PPG signals show that that HR can be accurately estimated from the PPG measurement, thus having the potential to become an alternative to ECG HR measurements in fish.

Based on the encouraging results from this experiment, the MAX86150 has been integrated with an inertial motion unit, a temperature and a magnetic field sensor in a stand-alone cylindrical implant measuring 13 × 40 mm [47]. This implant will undergo testing in swim tunnel trials logging motion data, ECG and PPG. Data from both wavelengths will be logged to evaluate the possibility of deriving *SpO2* from the data. These studies will enable the evaluation of how motion artefacts due to swimming motion impacts the data, and potentially how such artefacts can be remedied in post-processing.

Because this implant measures both ECG and PPG, co-processing of ECG and PPG for an even more robust HR estimate is made possible. This is already a topic in human medicine to improve accuracy and robustness for heart rate variability estimates beyond what is currently possible using ECG alone [48].

Acknowledgements

The authors thank the Research Council of Norway for funding the work (see “Funding”) as well as SINTEF Ocean AS for supporting the PhD project through their in-kind contribution. We also thank the personnel at NINA’s research station at lms for facilitating the experiment.

Authors’ contributions

ES and JAA conceived the idea for the setup and testing the sensing principle in fish. ES is responsible for the completion of the PhD in the funding project, designed the required equipment, planned and executed the experiment, prepared and processed data, and did the main job in preparing the manuscript. FØ participated in the planning and execution of the experiments with emphasis on anesthesia and surgery. MF, JAA assisted in equipment design and planning of the experiment. LLR has participated in data processing, while BF and REO have contributed with the anatomical and physiological considerations. All authors have provided feedback and contributed to writing the manuscript. All authors read and approved the final manuscript.

Funding

This study was funded by the Research Council of Norway (RCN Project Number 280864) and through in-kind from SINTEF Ocean.

Availability of data and materials

The data sets used and/or analysed during the current study are available from the corresponding author on reasonable request.

Declarations

Ethics approval and consent to participate

The animal experiment described herein was conducted with permission given by the Norwegian Food Safety Authority (permit number 19/104024). Permission to use up to, but not exceeding, 15 individual Atlantic salmon was given under the condition that data collection was stopped when 5 complete data sets were obtained as a reduction measure (3R) [49], a point that was reached after 7 fish. The experiment was carried out at NINA lms Research Station close to Stavanger, Norway, on August 28th, 2019.

Consent for publication

Not applicable.

Competing interests

The authors declare that they have no competing interests.

Author details

¹Department of Engineering Cybernetics, NTNU, O.S. Bragstads Plass 2D, 7034 Trondheim, Norway. ²Department of Aquaculture Technology, SINTEF Ocean, Brattørkaia 17C, 7010 Trondheim, Norway. ³Department of Electronic Systems, O.S. Bragstads Plass 2B, 7034 Trondheim, Norway. ⁴Norwegian Institute for Nature Research, Høgskoleringen 9, 7485 Trondheim, Norway. ⁵Department of Biology, NTNU, Brattørkaia 17B, 7010 Trondheim, Norway.

Received: 6 May 2021 Accepted: 13 September 2021

Published online: 22 September 2021

References

1. FAO: Food and Agriculture Organization of the United Nations, Fisheries and Aquaculture department (2021). <http://www.fao.org/fishery/aquaculture/en> Accessed 2 May 2021

2. Sommerset I, Walde C, Bang Jensen B, Bornø B, Haukaas A, Brun E. Fiskehelseberapporten 2019. report 5a/2020 (Norwegian Veterinary Institute, Oslo, Norway, 2019) (2020)
3. Noble C, Nilsson J, Stien LH, Iversen MH, Kolarevic J, Gismervik K. Velferdsindikatorer for oppdrettslaks: Hvordan vurdere og dokumentere fiskevelferd. 2. utgave (2018)
4. Føre M, Frank K, Norton T, Svendsen E, Alfredsen JA, Dempster T, Eguiraun H, Watson W, Stahl A, Sunde LM, et al. Precision fish farming: a new framework to improve production in aquaculture. *Biosys Eng.* 2017. <https://doi.org/10.1016/j.biosystemseng.2017.10.014>.
5. Knudsen F, Fosseidengen J, Oppedal F, Karlens Ø, Ona E. Hydroacoustic monitoring of fish in sea cages: target strength (ts) measurements on Atlantic salmon (*Salmo salar*). *Fish Res.* 2004;69(2):205–9.
6. Berckmans D. General introduction to precision livestock farming. *Anim Front.* 2017;7(1):6–11.
7. Føre M, Svendsen E, Alfredsen JA, Uglem I, Bloecher N, Sveier H, Sunde LM, Frank K. Using acoustic telemetry to monitor the effects of crowding and delousing procedures on farmed Atlantic salmon (*Salmo salar*). *Aquaculture.* 2018;495:757–65.
8. Brijs J, Sandblom E, Axelsson M, Sundell K, Sundh H, Huyben D, Broström R, Kiessling A, Berg C, Gräns A. The final countdown: continuous physiological welfare evaluation of farmed fish during common aquaculture practices before and during harvest. *Aquaculture.* 2018;495:903–911
9. Hassan W, Føre M, Pedersen, M.O., Alfredsen, J.A.: A novel doppler based speed measurement technique for individual free-ranging fish. In: 2019 IEEE SENSORS, pp. 1–4 (2019). IEEE
10. Baktoft H, Gjelland KØ, Økland F, Thygesen UH. Positioning of aquatic animals based on time-of-arrival and random walk models using yaps (yet another positioning solver). *Sci Rep.* 2017;7(1):1–10.
11. Hassan W, Føre M, Urke HA, Kristensen T, Ulvund JB, Alfredsen JA, et al. System for real-time positioning and monitoring of fish in commercial marine farms based on acoustic telemetry and internet of fish (iof). In: The 29th International Ocean and Polar Engineering Conference (2019). International Society of Offshore and Polar Engineers
12. Thorstad EB, Rikardsen AH, Alp A, Økland F. The use of electronic tags in fish research—an overview of fish telemetry methods. *Turk J Fish Aquat Sci.* 2013;13(5):881–96.
13. Deng ZD, Weiland MA, Fu T, Seim TA, LaMarche BL, Choi EY, Carlson TJ, Eppard MB. A cabled acoustic telemetry system for detecting and tracking juvenile salmon: Part 2. Three-dimensional tracking and passage outcomes. *Sensors.* 2011;11(6):5661–76. Doi: <https://doi.org/10.3390/s110605661>
14. Weiland MA, Deng ZD, Seim TA, LaMarche BL, Choi EY, Fu T, Carlson TJ, Thronas AI, Eppard MB. A cabled acoustic telemetry system for detecting and tracking juvenile salmon: Part 1. Engineering design and instrumentation. *Sensors.* 2011;11(6):5645–60. Doi: <https://doi.org/10.3390/s110605645>
15. Hussey NE, Kessel ST, Aarestrup K, Cooke SJ, Cowley PD, Fisk AT, Harcourt RG, Holland KN, Iverson SJ, Kocik JF et al. Aquatic animal telemetry: a panoramic window into the underwater world. *Science.* 2015;348(6240):1255642
16. Muñoz L, Aspillaga E, Palmer M, Saraiva JL, Arechavala-Lopez P. Acoustic telemetry: a tool to monitor fish swimming behavior in sea-cage aquaculture. *Front Marine Sci.* 2020;7: 645
17. Føre M, Frank K, Dempster T, Alfredsen JA, Høy E. Biomonitoring using tagged sentinel fish and acoustic telemetry in commercial salmon aquaculture: a feasibility study. *Aquacult Eng.* 2017;78:163–72.
18. Wendelaar Bonga SE. The stress response in fish. *Physiol Rev.* 1997;77(3):591–625.
19. Hvas M, Folkedal O, Oppedal F. Heart rate bio-loggers as welfare indicators in Atlantic salmon (*Salmo salar*) aquaculture. *Aquaculture.* 2020;529:735630.
20. Svendsen E, Føre M, Økland F, Gräns A, Hedger RD, Alfredsen JA, Uglem I, Rosten C, Frank K, Erikson U et al. Heart rate and swimming activity as stress indicators for Atlantic salmon (*Salmo salar*). *Aquaculture.* 2020;531: 735804
21. Brijs J, Sandblom E, Rosengren M, Sundell K, Berg C, Axelsson M, Gräns A. Prospects and pitfalls of using heart rate bio-loggers to assess the welfare of rainbow trout (*Oncorhynchus mykiss*) in aquaculture. *Aquaculture.* 2019;509:188–197

22. Charlton PH, Birrenkott DA, Bonnici T, Pimentel MA, Johnson AE, Alastruey J, Tarassenko L, Watkinson PJ, Beale R, Clifton DA. Breathing rate estimation from the electrocardiogram and photoplethysmogram: a review. *IEEE Rev Biomed Eng.* 2017;1:2–20.
23. Severinghaus JW. Takuo aoyagi: discovery of pulse oximetry. *Anesth Analg.* 2007;105(6):1–4.
24. Chan ED, Chan MM, Chan MM. Pulse oximetry: understanding its basic principles facilitates appreciation of its limitations. *Respir Med.* 2013;107(6):789–99.
25. Islam MT, Zabir I, Ahamed ST, Yasar MT, Shahnaz C, Fattah SA. A time-frequency domain approach of heart rate estimation from photoplethysmographic (ppg) signal. *Biomed Signal Process Control.* 2017;36:146–54.
26. Erhardt W, Lendl C, Hipp R, von Hegel G, Wiesner G, Wiesner H. The use of pulse oximetry in clinical veterinary anaesthesia. *J Assoc Vet Anaesth Great Br Irel.* 1990;17(1):30–1. <https://doi.org/10.1111/j.1467-2995.1990.tb00385.x>.
27. Theodor M, Ruh D, Subramanian S, Förster, K, Heilmann C, Beyersdorf F, Plachta D, Manoli Y, Zappe H, Seifert A. Implantable pulse oximetry on subcutaneous tissue. In: 2014 36th Annual International Conference of the IEEE Engineering in Medicine and Biology Society, pp. 2089–2092 (2014). IEEE
28. Reynolds J, Ahmmed P, Bozkurt A. An injectable system for subcutaneous photoplethysmography, accelerometry, and thermometry in animals. *IEEE Trans Biomed Circuits Syst.* 2019;13(5):825–34.
29. Machikhin AS, Burlakov AB, Volkov MV, Khokhlov DD. Imaging photoplethysmography and videocapillaroscopy enable noninvasive study of zebrafish cardiovascular system functioning. *J Biophotonics.* 2020;13(7):202000061.
30. Seo E, Sazi T, Togawa M, Nagata O, Murakami M, Kojima S, Seo Y. A portable infrared photoplethysmograph: heartbeat of *Mytilus galloprovincialis* analyzed by mri and application to bathymodiolus septemdiemur. *Biol Open.* 2016;5(11):1752–7.
31. Tomlinson S, Behrmann S, Cranford J, Louie M, Hashikawa A. Accuracy of smartphone-based pulse oximetry compared with hospital-grade pulse oximetry in healthy children. *Telemed e-Health.* 2018;24(7):527–35. <https://doi.org/10.1089/tmj.2017.0166>.
32. Hahnen C, Freeman CG, Haldar N, Hamati JN, Bard DM, Murali V, Merli GJ, Joseph JI, van Helmond N. Accuracy of vital signs measurements by a smartwatch and a portable health device: validation study. *JMIR Mhealth Uhealth.* 2020;8(2):16811.
33. Maxim Integrated: Maxim Integrated, Integrated Photoplethysmogram and Electrocardiogram Bio-sensor Module for Mobile Health (2021). <https://datasheets.maximintegrated.com/en/ds/MAX86150.pdf> Accessed 9 Aug 2021.
34. Coyle SD, Durborow RM, Tidwell JH, et al. Anesthetics in aquaculture vol. 3900. Southern Regional Aquaculture Center, Stoneville (2004)
35. Elgendi M. Optimal signal quality index for photoplethysmogram signals. *Bioengineering.* 2016;3(4):21. <https://doi.org/10.3390/bioengineering3040021>.
36. Doving K, Reimers E. *Fiskens Fysiologi*. Bergen: John Grieg; 1992
37. Lucas M. Heart rate as an indicator of metabolic rate and activity in adult Atlantic salmon, *Salmo salar*. *J Fish Biol.* 1994;44(5):889–903.
38. Butterworth C. Filter approximation theory. *Engineer.* 1930;7:536–41.
39. Savitzky A, Golay MJ. Smoothing and differentiation of data by simplified least squares procedures. *Anal Chem.* 1964;36(8):1627–39.
40. Farrell AP. *Encyclopedia of fish physiology: from genome to environment*. London: Academic press; 2011.
41. Johns M, Giller CA, German DC, Liu H. Determination of reduced scattering coefficient of biological tissue from a needle-like probe. *Opt Express.* 2005;13(13):4828–42.
42. Bigio, I.J., Fantini, S.: *Quantitative Biomedical Optics: Theory, Methods, and Applications*. Cambridge University Press, University Printing Press, Cambridge CB2 8BS, United Kingdom (2016)
43. Nitzan M, Khanokh B, Slovik Y. The difference in pulse transit time to the toe and finger measured by photoplethysmography. *Physiol Meas.* 2001;23(1):85.
44. Golyandina N, Zhigljavsky A. *Singular spectrum analysis for time series*, vol. 120. Heidelberg New York Dordrech London: Springer; 2013.
45. Meyer Y. *Wavelets: algorithms & applications*. Philadelphia: SIAM (Society for Industrial and Applied Mathematics; 1993.
46. Cooley JW, Tukey JW. An algorithm for the machine calculation of complex fourier series. *Math Comput.* 1965;19(90):297–301.
47. Svendsen E, Førre M, Randeberg L, JA., Design of a novel biosensor implant for farmed Atlantic salmon (*Salmo salar*). In: 2021 IEEE SENSORS, Accepted for Publication (2021). IEEE
48. Zaretskiy A, Mityagin K, Tarasov V, Moroz D, Kuraleva A. Robust heart rate estimation using combined ecg and ppg signal processing. In: IOP Conference Series: Materials Science and Engineering, vol. 537, p. 042077 (2019). IOP Publishing
49. Norecopa: Norecopa, Norway's National Consensus Platform (2021). <https://norecopa.no/> Accessed 10 Mar 2021

Publisher's Note

Springer Nature remains neutral with regard to jurisdictional claims in published maps and institutional affiliations.

Ready to submit your research? Choose BMC and benefit from:

- fast, convenient online submission
- thorough peer review by experienced researchers in your field
- rapid publication on acceptance
- support for research data, including large and complex data types
- gold Open Access which fosters wider collaboration and increased citations
- maximum visibility for your research: over 100M website views per year

At BMC, research is always in progress.

Learn more biomedcentral.com/submissions

